CHEMISTRY
A EUROPEAN JOURNAL

DOI: 10.1002/chem.201001261

Growing Au/Ag Nanoparticles within Microgel Colloids for Improved Surface-Enhanced Raman Scattering Detection

Rafael Contreras-Cáceres,[a, b] Isabel Pastoriza-Santos,[a] Ramón A. Alvarez-Puebla,[a] Jorge Pérez-Juste,*[a] Antonio Fernández-Barbero,[b] and Luis M. Liz-Marzán*[a]

The synthesis, characterization, and assembly of different types of nanoparticles, which was established as a necessary prerequisite for the application of nanotechnology, have dramatically advanced over the last 20 years.[1,2] However, it has recently been realized that the incorporation of multiple functionalities within nanoscale systems would become much more useful for most of the foreseen applications. Thus, the fabrication of multifunctional nanoparticles has become a major challenge. Among these systems, the incorporation of active (optically, catalytically, magnetically…) nanoparticles within so-called "smart" thermosensitive microgels has received significant attention over the last few years.[3,4] The incorporation of nanoparticles can be accomplished either by in situ formation, by post-synthesis assembly or by direct polymerization on the nanoparticles surface.[5,6] We have recently reported the growth of thermosensitive poly(*N*-isopropylacrylamide) (pNIPAM) microgels on the surface of gold nanoparticles, involving several steps, including the formation of a first polystyrene thin layer, followed by pNIPAM polymerization after the required purification process.[7,8] Although gold nanoparticle growth could be achieved within the microgel shell, this synthesis was restricted to spherical nanoparticle seeds, whereas, for example, nanorods (which display a much more interesting optical response) were not properly incorporated. Thus, there was a need to both simplify the coating process and make it more widely applicable.

We report here a novel procedure where butenoic acid is used for the synthesis of gold nanoparticles in aqueous surfactant solutions, in the presence of preformed Au seeds. Apart from the interesting observation that butenoic acid can be used as a reducing agent, this is particularly interesting because it provides the particles with a vinyl functionality, which should be useful for the direct pNIPAM polymerization on the nanoparticles surface and their subsequent encapsulation, while avoiding complicated surface functionalization steps. Although we have only optimized the reduction process for nanosphere growth, we also demonstrate that butenoic acid can replace cetyltrimethylammonium bromide (CTAB) molecules from Au nanoparticle surfaces, including Au nanorods, and adsorb on the metal surface, thereby facilitating the polymerization of pNIPAM on the metal core. The improved stability of the nanocomposites and the porosity of the pNIPAM shell allows subsequent reduction of metal atoms on the metal core, which was exploited for the overgrowth of pNIPAM encapsulated Au spheres and rods with both Au and Ag under mild conditions. In a previous publication[9] we demonstrated the ability of these composite colloids to mechanically trap non-common surface-enhanced Raman scattering (SERS) analytes. However, the use of 60 nm gold spheres as colloidal cores and the impossibility of forming hot spots due to the physical barrier imposed by the pNIPAM shell severely limited the enhancing capability and thus the detection limit. In the present work, the SERS intensity was significantly increased through manipulation of the composition and the morphology of the nanoparticle cores. Thus, the first modification involved the controlled growth of uniform silver shells, a much more efficient plasmonic material,[10] on the gold cores. Second, we exploited the near field concentration at the ends of nanorods to further increase the signal.[11,12] Finally, we demonstrate that the molecular affinity of the pNIPAM shells toward analytes can be extended by tuning the surface charge, which would allow the electrostatic attraction of charged molecules.[13,14]

[a] R. Contreras-Cáceres, Dr. I. Pastoriza-Santos,
Dr. R. A. Alvarez-Puebla, Dr. J. Pérez-Juste, Prof. L. M. Liz-Marzán
Departamento de Química Física, and Unidad Asociada CSIC
Universidade de Vigo, 36310, Vigo (Spain)
Fax: (+34) 986812556
E-mail: juste@uvigo.es
lmarzan@uvigo.es

[b] R. Contreras-Cáceres, Prof. A. Fernández-Barbero
Departamento de Física Aplicada
Universidad de Almería
Almería (Spain)

Supporting information for this article is available on the WWW under http://dx.doi.org/10.1002/chem.201001261.

It has been reported that spherical Au nanoparticles in a wide size range can be prepared in aqueous solutions of the cationic surfactant CTAB, through a seeded growth method in which an ionic precursor is catalytically reduced by ascorbic acid, a mild reducing agent, on preformed Au seeds.[15,16] Other organic acids such as salicylic acid[17] have also been reported to show similar reducing capabilities, so that they can reduce Au^{III}–CTAB complexes to Au^{I}–CTAB but reduction into Au^0 can only take place on catalytic metallic gold surfaces. Recently, Xia and co-workers have shown the reducing capability of the vinyl group toward $HAuCl_4$, in the presence of water, so that gold nanoparticles could be formed.[18] Considering that butenoic acid presents both a vinyl and an acidic group, it was expected to display an enhanced reduction power for the gold salt precursor.

The results obtained using butenoic acid as reducing agent have been found to be similar to those reported for ascorbic acid, but our interest was related to the adsorption of additional butenoic acid molecules, added in excess, onto the particles surface, through the carboxylic group, providing the particles with the vinyl functionality.[19] Therefore, upon removal of the excess CTAB, nanoparticles grown with butenoic acid might be directly used for their encapsulation with pNIPAM, avoiding any additional functionalization. Figure S1 in the Supporting Information shows a representative TEM image of approximately 64 nm diameter gold nanoparticles prepared through overgrowth of 15 nm Au seeds by $HAuCl_4$ reduction with butenoic acid, in the presence of CTAB. Encapsulation within pNIPAM shells was achieved by simply removing the excess CTAB and adding the NIPAM monomer, a crosslinker and an initiator (see Experimental Section). A representative TEM image of the same gold nanoparticles coated with pNIPAM (Au@pNIPAM) is shown in Figure S2 in the Supporting Information. It is clear from these images that all the particles are perfectly encapsulated in the pNIPAM shell, which indicates that the vinyl groups present on the particles promote uniform pNIPAM polymerization over the whole surface of the nanoparticles, as has been previously shown for gold and silica.[7,20,21] Although the use of butenoic acid in the reduction process is convenient, it can also be adsorbed on CTAB-capped gold particles, which allows to carry out the pNIPAM encapsulation of other preformed nanoparticles with interesting morphologies, such as nanorods. In this case, a suitable amount of butenoic acid (see Experimental Section) was added to the Au nanorod colloids and allowed to equilibrate for 1 h, prior to starting the polymerization of pNIPAM. The result was an extremely efficient coverage of all the Au nanorods within pNIPAM microgel spheres, as revealed by the corresponding TEM images (see Figure S3 in the Supporting Information). Apart from the interest of coating nanorods, the success of this approach confirms the capability of butenoic acid to adsorb onto Au particles, in the presence of CTAB, and still serve as anchor points for pNIPAM.

We have reported,[7,8] that both the size and the plasmonic response of pNIPAM-based metal nanocomposites can be tuned with temperature and are fully reversible. We registered the changes in hydrodynamic diameter and position of the localized surface plasmon resonance (LSPR) with temperature for both Au-sphere(64 nm)@pNIPAM and Au-nanorod@pNIPAM nanocomposite colloids (see Figure S2 and S3 in the Supporting Information). The photon correlation spectroscopy (PCS) data revealed that the lower critical solution temperature (LCST) of the pNIPAM shells is similar to that reported for pure microgels,[22] while the LSPR bands of the aqueous dispersions are consistently redshifted as the microgel shell collapses due to the increase in local refractive index around the metal core.[23,24] As expected, the variation of the LSPR position with temperature can be nicely correlated to the variation of the hydrodynamic diameter. It should also be pointed out that a larger LSPR shift was recorded for Au-nanorod@pNIPAM than for Au-sphere(64 nm)@pNIPAM (21 nm vs. 11 nm), mainly because of a higher electromagnetic field concentration in nanorods than in spheres, which also leads to a higher sensitivity toward local refractive index changes.[25]

A major advantage of the efficient encapsulation of gold nanoparticles with pNIPAM arises from the high porosity of the shell and the high colloidal stability, so that chemical reactions can be carried out while aggregation is completely avoided.[26] Interesting reactions are related to the possibility of post-coating reduction of metals on the gold cores, which allows not only adjusting their size[8] but also their composition if different metals are used.[24] One obvious choice in the context of plasmonic applications is the growth of silver on the pre-encapsulated gold cores. Silver is significantly more efficient than gold as a plasmonic metal because its interband transitions are restricted to the UV, but the synthesis of size- and shape-controlled silver nanoparticles is more complicated than for gold. Thus, it is advantageous to use preformed gold nanoparticles as templates for the preparation of silver shells with various morphologies,[27–29] which display optical properties close to those of pure silver. In this context, we decided to attempt the in situ growth of silver shells on the Au cores for the Au-sphere(64 nm)@pNIPAM and Au-nanorod@pNIPAM composite colloids. The coating process simply involved the reduction of $AgNO_3$ with ascorbic acid, in the presence of the corresponding core–shell colloids. As a blank for comparison, we also carried out the growth of the same starting particles with additional gold, in the same molar proportion as for silver. Figure 1 A and C show representative TEM images of the particles grown with Au (spheres and rods, respectively), whereas Figure 1 B and D show the result of growing silver shells on the same cores, resulting in Au@Ag core@shell metal nanoparticles, covered with pNIPAM. The insets in Figure 1 B and 1D show the typical intensity contrast between the Au core and the Ag shell (due to the electron scattering differences between both metals), clearly revealing the uniform coating for both geometries. Interestingly, these new, core-grown, nanocomposites retain the original thermoresponsive properties of the polymer shell. Figures S4–S7 in the Supporting Information show that in all

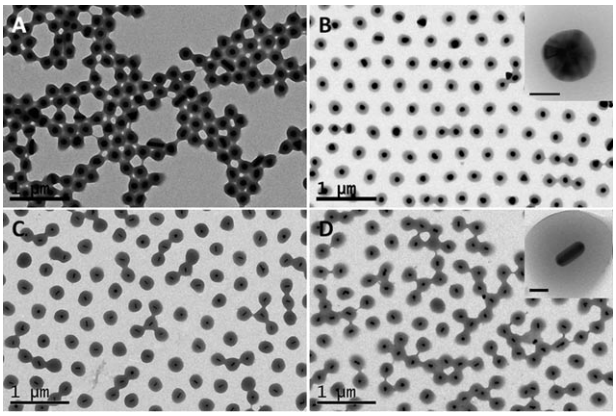

Figure 1. Representative TEM images of metal@pNIPAM nanocomposites with different cores; A) 103 nm Au, B) Au(64 nm)@Ag(18 nm) core@shell, C) gold nanorods ((82.1±7.9) nm × 21.6±2.6), and D) Au@Ag core@shell nanorods ((76.7±7.7) nm × 40.0±5.1). The scale bar in the insets is 50 nm.

cases the overall dimensions, measured by PCS, are similar before and after the various core growth experiments. Figure 2 summarizes the optical properties of the aqueous

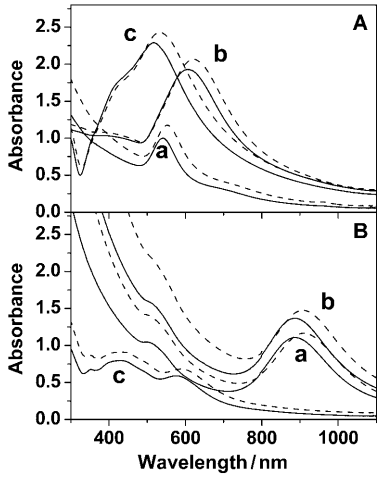

Figure 2. UV/Vis-NIR spectra of the different metal@pNIPAM aqueous composite colloids, below (22 °C, solid lines) and above (44 °C, dashed lines) the LCST; A) 64 nm Au spheres (a), 103 nm Au spheres (b), and 100 nm Au@Ag (64/18) core–shells (c). B) Au nanorod (a), Au@Au nanorod (b), and Au@Ag nanorod (c).

dispersions of the different nanocomposites. The first observation is that, while the growth of Au spherical cores from 64 to 103 nm leads to a significant redshift because of retardation effects,[16] coating with Ag up to a total diameter of 100 nm results in a clear blueshift and formation of a quadrupolar mode, in agreement with previous reports.[30] On the other hand, the growth of gold nanorod cores was uniform, with only a slight decrease of the aspect ratio, so that the LSPR bands only changed in intensity. However, the optical changes derived from silver growth were more remarkable, not only due to the presence of silver on the surface, but also because the growth took place preferentially at the sides, in agreement with recent reports for gold rods in solution.[27,29] These two effects lead to a dramatic blueshift of the longitudinal LSPR, so that it is strongly affected by the Rayleigh scattering arising from the pNIPAM shell. Regarding the reversible thermoresponsive behavior of the optical properties for the different composite colloids, it can be summarized through the total redshift of the LSPR at high temperature (above the LCST at 32 °C) due to the collapse of the polymer shell. The maximum value of the redshift depends on the metal core size, shape, and composition, since these three factors are known to dominate the LSPR sensitivity toward changes in the local refractive index.[25,31] As an example, the LSPR shift for spherical nanoparticles varies from 10 nm for Au-sphere(64 nm)@pNIPAM, to 17 nm for Au(64 nm)@Ag@pNIPAM, and up to 28 nm for the thicker gold nanorods. Unfortunately, the scattering overlap does not allow us to make a proper observation of the LSPR shifts in Au-nanorod@Ag@pNIPAM, though a redshift was also observed.

The SERS efficiency of the different materials was characterized by recording spectra of 1-naphthalenethiol (1NAT), which is a non-resonant molecule in both the visible and the IR. As shown in Figure 3 (inset), the SERS spectra of 1NAT are characterized by ring stretching (1553, 1503, and 1368 cm^{-1}), CH bending (1197 cm^{-1}), ring breathing (968 and 822 cm^{-1}), ring deformation (792, 664, 539, and 517 cm^{-1}), and CS stretching (389 cm^{-1}), in agreement with

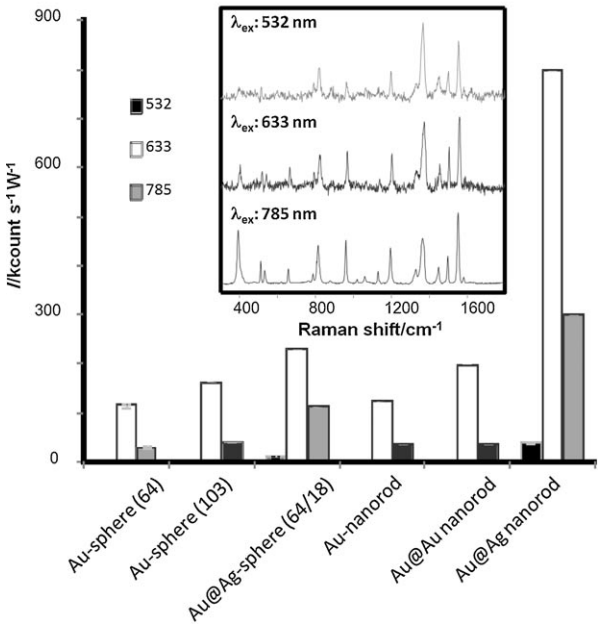

Figure 3. Comparison of the intensities of the ring stretching peak (1368 cm^{-1}) for the different samples, acquired in solution upon excitation with 532, 633, and 785 nm laser lines. The intensities are normalized for the same amount of particles in each suspension. Inset: Representative average SERS spectra of 1NAT in pNIPAM-coated metal colloids, acquired upon excitation with the different laser lines.

previous reports.[32] From Figure 3, one can see that all our systems provided sufficient enhancement to allow identification of 1NAT from solution, thus confirming that the molecules can diffuse through the porous shells and reach the metallic cores, where they bind through the thiol group. Note that three different laser lines were used for excitation, so that coupling to the respective LSPR modes was possible for all different samples. The morphological and chemical modification of the particles in the present study allowed us to compare the effect of different parameters on the detection capabilities of the composites. For both spheres and rods, the SERS intensity was found to increase with core size, but the differences were modest as compared with those originated by the presence of silver. Additionally, the spectral changes dictated by the silver coating allowed us to use the green laser line (532 nm), which is very inefficient in pure gold particles due to damping by interband transitions. On the other hand, changes in shape from spheres to rods greatly affected the recorded SERS intensity. This was particularly important for the case of silver-coated nanorods, where silver not only increases the optical efficiency but blueshifts the longitudinal LSPR, which leads to strong electric field concentration at the ends of the rods.[11,12] The net effect is a substantial increase in the SERS intensity recorded from the Au-nanorod@Ag@pNIPAM sample, upon excitation with the red laser (633 nm).

Apart from 1NAT, which can easily bind to the metal cores through the thiol group, we demonstrate here the possibility of using this composite system for electrostatic trapping of charged analytes. To this end, we added to a small volume of the Au-nanorod@Ag@pNIPAM colloid a dilute alkaline solution of 2-naphthoic acid (2NA, pH 13). The final pH of the suspension was 11, at which 2NA is completely ionized and is thus very unlikely to adsorb on standard, citrate-stabilized silver colloids, which also have negative surface charge. This was confirmed when 2NA was mixed with a citrate–Ag colloid and a totally featureless SERS spectrum was recorded, as shown in Figure 4. However, since the pNIPAM shells were grown using a cationic initiator (AAPH), they display a positive surface charge (+25 mV), which is expected to be present not only at the outer surface but also within the pores, so that 2NA anions can adsorb on the shell, giving rise to a significant increase in the recorded SERS intensity. All pNIPAM composites yielded SERS, as demonstrated through the well-defined spectra for 2NA (Figure 4), dominated by the ring stretchings at 1632 and 1388 cm^{-1}, CH bending at 1468 cm^{-1}, ring breathing at 1018 cm^{-1}, and CH deformation at 770 cm^{-1}.[14] However, and consistent with the previous findings, composites prepared with gold and silver with rod shape provided a substantially larger intensity, demonstrating again their suitability for SERS analysis even when the formation of hot spots is inhibited.

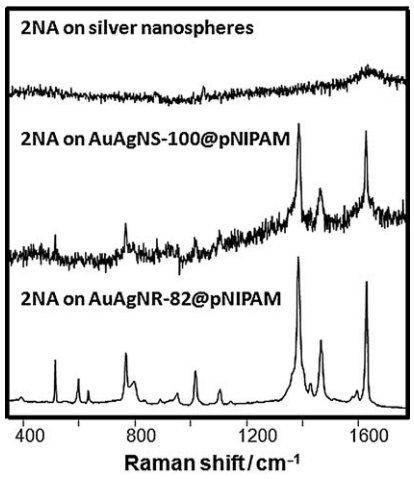

Figure 4. SERS spectra of an alkaline solution of 2-naphthoic acid on different colloidal suspensions. Excitation laser line was 633 nm.

In summary, we have demonstrated that the use of butenoic acid largely facilitates the surface polymerization of pNIPAM shells on a variety of gold nanoparticles, which can be further manipulated within the porous shells, either to increase their size or to grow silver shells, thereby significantly improving their plasmonic performance. The Au@Ag@pNIPAM colloids were found to provide much higher SERS intensities than their Au@pNIPAM counterparts, not only in the case of spheres but particularly for nanorods. Additionally, the tunable surface charge of the microgels can be exploited to adsorb different types of analyte molecules and generalize the use of these systems for SERS detection.

Experimental Section

Materials: Ascorbic acid (AA), hydrochloric acid, cetyltrimethylammonium bromide (CTAB), butenoic acid, silver nitrate ($AgNO_3$), sodium borohydride ($NaBH_4$), *N*-isopropylacrylamide (NIPAM, 97%), and 2-naphthoic acid (2NA) were supplied by Aldrich. $HAuCl_4{\cdot}3H_2O$, trisodium citrate dihydrate and sodium hydroxide (NaOH) were supplied by Sigma. *N,N′*-Methylenebisacrylamide (BIS) was supplied by Fluka. 2,2′-Azobis(2-methylpropionamidine) dihydrochloride (AAPH) and 1-naphthalenethiol (1NAT) were supplied by Acros Organics. All reactants were used without further purification. Water was purified using a Milli-Q system (Millipore).

Au-sphere(64 nm)@pNIPAM particles: Au seeds (64 nm) were prepared through a seeded growth method. Briefly, 35 mL of approximately 15 nm Au nanoparticles (previously prepared by citrate reduction) was added to 15 mL of 0.03 M CTAB aqueous solution. A 4.5 mL portion of this seed solution was added to a growth solution prepared by adding butenoic acid (800 μL) under gentle stirring to 50 mL of an aqueous solution containing 1 mM $HAuCl_4$ and 15 mM CTAB at 70 °C. After 10 min, excess butenoic acid and CTAB were removed by centrifugation at 4500 rpm for 30 min. After redispersing the pellet in 4 mM CTAB (50 mL), the dispersion was centrifuged at 4500 rpm for 40 min and the precipitate redispersed in water (10 mL). Subsequently this Au colloidal dispersion was heated at 70 °C under N_2 flow and then NIPAM (0.1698 g) and BIS (0.0234 g) were added under magnetic stirring. After 15 min, the nitrogen flow was removed and the polymerization was initiated with the addition of AAPH (100 μL 0.1 M). After 2 h at 70 °C, the white mixture was allowed to cool down to room temperature under stirring. Finally, it was diluted with water (50 mL), centrifuged (30 min at 4500 rpm) and redispersed in water (fivefold). The Au core size measured from TEM was (63.9 ± 5.9) nm.

Au-sphere(103 nm)@pNIPAM: The growth of the Au core was carried out following the method developed by Rodríguez-Fernández et al.[16]

Briefly, to 10 mL of an aqueous solution containing Au-sphere-(64 nm)@pNIPAM (0.25 mM), CTAB (0.1 M), and $HAuCl_4$ (0.9 mM), 180 μL of AA 0.1 M was added under magnetic stirring. After 30 min the growth process was finished. The Au core size measured from TEM was (103.0 ± 8.4) nm.

Au-sphere(64 nm)@Ag@pNIPAM: The coating of 64 nm Au cores with Ag was carried out following the method developed by Yang et al.[33] To 10 mL of 0.4 M glycine buffer solution at pH 9.5 containing Au-sphere-(64 nm)@pNIPAM (0.25 mM) and CTAB (50 mM), first 655 μL of 15.2 mM $AgNO_3$ aqueous solution and subsequently 450 μL of AA 0.1 M were added. After 30 min the reduction was finished. The Au@Ag core size measured from TEM was (100.3 ± 9.2) nm.

Au-nanorod@pNIPAM: Gold nanorod colloid (250 mL) was synthesized by using the seed-mediated synthesis reported by Guyot-Sionnest et al.[34] The dimensions of the obtained nanorods measured from TEM were (70.0 ± 7.2) nm × (17.6 ± 3.1) nm (aspect ratio, AR = 4.1 ± 0.8). Then, 100 mL of the gold nanorod colloid was centrifuged at 7000 rpm for 1 h to remove excess CTAB and redispersed in water (100 mL). Then, pure butenoic acid (300 μL) was added to the nanorod solution at 70 °C. After 1 h, the dispersion was centrifuged (1 h at 6000 rpm) to remove the butenoic acid in excess and the pellet was redispersed in water (10 mL). pNIPAM encapsulation was carried out as explained above for Au-sphere(64 nm)@Ag@pNIPAM particles. The only changes were the amounts of NIPAM (0.1924 g), BIS (0.0265) and AAPH (100 μL 0.1 M) used. After polymerization, the dispersion was diluted with water (50 mL), centrifuged (1 h at 5500 rpm) and redispersed in water fivefold).

Growth of Au-nanorod@pNIPAM (Au-nanorod@Au@pNIPAM): This was carried out as described above for Au-sphere(64 nm)@Au@pNIPAM, but using 0.8 mM $HAuCl_4$ and 160 μL of 0.1 M AA. The final Au core size measured from TEM was (82.1 ± 7.9) nm × (21.6 ± 2.6) nm (AR = 3.6 ± 0.5).

Au-nanorod@Ag@pNIPAM: The process was as described above for Au-sphere(64 nm)@Ag@pNIPAM, changing the amounts of $AgNO_3$ (540 μL of 14.83 mM) and AA (360 μL 0.1 M) aqueous solutions. The final core size measured by TEM was (76.7 ± 7.7) nm × (40.0 ± 5.1) nm (AR = 1.9 ± 0.4).

Characterization: UV/Vis-NIR spectra were recorded by using a Cary 5000 spectrophotometer. Transmission electron microscopy (TEM) was performed in a JEOL JEM 1010 microscope operating at an acceleration voltage of 100 kV. Photon correlation spectroscopy (PCS) was carried out on a Zetasizer Nano S (Malvern Instruments, Malvern UK) using a detection angle of 173°. The intensity-averaged particle diameter and the polydispersity index values were calculated from cumulant-type analysis.

SERS measurements: Samples for SERS were prepared by adding 15 μL of either an ethanol 1NAT solution or an aqueous alkaline solution (pH 13) 2NA both 10^{-3} M to 1.5 mL of each sample (Au-sphere-(64 nm)@pNIPAM, Au-sphere(103 nm)@pNIPAM, Au-sphere-(64 nm)@Ag@pNIPAM, Au-nanorod@pNIPAM, Au-nanorod@Au@pNIPAM and Au-nanorod@Ag@pNIPAM). After 1 h, allowing for thermodynamic equilibrium to be reached, average SERS was directly recorded from these suspensions. The inelastically scattered radiation was collected with a Renishaw Invia system, equipped with Peltier charge-coupled device (CCD) detectors and a Leica confocal microscope. The spectrograph has 1800 or 1200 g mm^{-1} gratings with additional band-pass filter optics. Samples were excited with three different laser lines at 532 (Nd:YAG), 633 nm (He-Ne) and 785 nm (diode). Spectra were collected in Renishaw extended mode with accumulation times of 10 s using a macrosampling 90° objective adaptor.

Acknowledgements

R.C.-C. acknowledges Junta de Andalucía for a PhD Scholarship (project FQM-02353). This work was supported by the Spanish Ministerio de Ciencia e Innovación/FEDER (grants MAT2007-62696, MAT2008-05755, and Consolider Ingenio 2010-CSD2006-12), Xunta de Galicia (PGIDIT06TMT31402PR and 08TMT008314PR), and the EU (INGENIOUS, grant number CP-248236).

Keywords: colloids · gold · nanoparticles · microgels · Raman spectroscopy · silver

[1] C. Burda, X. Chen, R. Narayanan, M. A. El-Sayed, *Chem. Rev.* **2005**, *105*, 1025–1102.
[2] M.-C. Daniel, D. Astruc, *Chem. Rev.* **2004**, *104*, 293–346.
[3] M. A. C. Stuart, W. S. Huck, J. Genzer, M. Müller, C. Ober, M. Stamm, G. B. Sukhorukov, I. Szleifer, V. V. Tsukruk, M. Urban, F. Winnik, S Zauscher, Igor Luzinov, S. Minko, *Nat. Mater.* **2010**, *9*, 101–113.
[4] S. Nayak, L. A. Lyon, *Angew. Chem.* **2005**, *117*, 7862–7886; *Angew. Chem. Int. Ed.* **2005**, *44*, 7686–7708.
[5] M. Karg, T. Hellweg, *Curr. Opin. Colloid Interface Sci.* **2009**, *14*, 438–450.
[6] A. Fernández-Barbero, I. J. Suárez, B. Sierra-Martín, A. Fernández-Nieves, F. Javier de Las Nieves, M. Marquez, J. Rubio-Retama, E. López-Cabarcos, *Adv. Colloid Interface Sci.* **2009**, *147–148*, 88–108.
[7] R. Contreras-Cáceres, A. Sánchez-Iglesias, M. Karg, I. Pastoriza-Santos, J. Pérez-Juste, J. Pacifico, T. Hellweg, A. Fernández-Barbero, L. M. Liz-Marzán, *Adv. Mater.* **2008**, *20*, 1666–1670.
[8] R. Contreras-Cáceres, J. Pacifico, I. Pastoriza-Santos, J. Pérez-Juste, A. Fernández-Barbero, L. M. Liz-Marzán, *Adv. Funct. Mater.* **2009**, *19*, 3070–3076.
[9] R. A. Álvarez-Puebla, R. Contreras-Cáceres, I. Pastoriza-Santos, J. Pérez-Juste, L .M. Liz-Marzán *Angew. Chem.* **2009**, *121*, 144–149; *Angew. Chem. Int. Ed.* **2009**, *48*, 138–143.
[10] J. Zhao, A. O. Pinchuk, J. M. McMahon, S. Li, L. K. Ausman, A. L. Atkinson, G. C. Schatz, *Acc. Chem. Res.* **2008**, *41*, 1710–1720.
[11] W. Cai, R. Sainidou, J. Xu, A. Polman, F. J. García de Abajo, *Nano Lett.* **2009**, *9*, 1176–1181.
[12] E. J. R. Vesseur, R. de Waele, M. Kuttge, A Polman, *Nano Lett.* **2007**, *7*, 2843–2846.
[13] R. A. Alvarez-Puebla, E. Arceo, P. J. G. Goulet, J. J. Garrido, R. F. Aroca, *J. Phys. Chem. B* **2005**, *109*, 3787–3792.
[14] R. A. Alvarez-Puebla, R. F. Aroca, *Anal. Chem.* **2009**, *81*, 2280–2285.
[15] N. R. Jana, L. Gearheart, C. J. Murphy, *Langmuir* **2001**, *17*, 6782–6786.
[16] J. Rodríguez-Fernández, J. Pérez-Juste, F. J. García de Abajo, L. M. Liz-Marzán, *Langmuir* **2006**, *22*, 7007–7010.
[17] S. Okamoto, S. Hachisu, *J. Colloid Interface Sci.* **1977**, *62*, 172–181.
[18] M. S. Yavuz, W. Li, Y. Xia, *Chem. Eur. J.* **2009**, *15*, 13181–13187.
[19] S. H. Han, S. W. Joo, T. H. Ha, Y. Kim, K. Kim, *J. Phys. Chem. B* **2000**, *104*, 11987–11995.
[20] L. Zha, Y. Zhang, W. Yang, S. Fu, *Adv. Mater.* **2002**, *14*, 1090.1092.
[21] M. Karg, I. Pastoriza-Santos, L. M. Liz-Marzán, T. Hellweg, *ChemPhysChem* **2006**, *7*, 2298–2301.
[22] K. Kratz, T. Hellweg, W. Eimer, *Polymer* **2001**, *42*, 6631.
[23] M. Karg, I. Pastoriza-Santos, J. Pérez-Juste, T. Hellweg, L. M. Liz-Marzán, *Small* **2007**, *3*, 1222–1229.
[24] A. Sánchez-Iglesias, M. Grzelczak, B. Rodríguez-González, P. Guardia-Girós, I. Pastoriza-Santos, J. Pérez-Juste, M. Prato, L. M. Liz-Marzán, *ACS Nano* **2009**, *3*, 3184–3190.
[25] H. Chen, X. Kou, Z. Yang, W. Ni, J. Wang, *Langmuir* **2008**, *24*, 5233–5237.
[26] S. Carregal-Romero, N. J. Buurma, J. Pérez-Juste, P. Hervés, L. M. Liz-Marzán, *Chem. Mater*, **2010**, *22*, 3051–3059.
[27] A. Sánchez-Iglesias, E. Carbó-Argibay, A. Glaria, B. Rodríguez-González, J. Pérez-Juste, I. Pastoriza-Santos, L. M. Liz-Marzán, *Chem. Eur. J.* **2010**, *16*, 5558–5563.
[28] E. C. Cho, P. H. C. Camargo, Y. Xia, *Adv. Mater.* **2010**, *22*, 744–748.
[29] Y. Xiang, X. Wu, D. Liu, Z. Li, W. Chu, L. Feng, K. Zhang, W. Zhou, S. Xie, *Langmuir* **2008**, *24*, 3465–3470.

[30] B. Rodríguez-González, A. Burrows, M. Watanabe, C. J. Kiely, L. M. Liz-Marzán, *J. Mater. Chem.* **2005**, *15*, 1755–1759.
[31] B. Sepúlveda, P. C. Angelomé, L. M. Lechuga, L. M. Liz-Marzán, *Nano Today* **2009**, *4*, 244–251.
[32] R. A. Álvarez-Puebla, D. S. Dos Santos, Jr., R. F. Aroca, *Analyst* **2004**, *129*, 1251–1256.
[33] Z. Yang, Y.-W. Lin, W.-L. Tseng, H.-T. Chang, *J. Mater. Chem.* **2005**, *15*, 2450–2454.
[34] M. Liu, P. Guyot-Sionnest, *J. Phys. Chem. B* **2005**, *109*, 22192–22200.

Received: May 10, 2010
Published online: July 19, 2010

